In vivo imaging of inflammation using an aptamer inhibitor of human neutrophil elastase

Josephine Charlton, Joseph Sennello and Drew Smith

Background: We previously reported the isolation of aptamer irreversible inhibitors of human neutrophil elastase. We now report on the application of aptamer technology to the field of diagnostic imaging.

Results: The enzyme elastase has been reported to bind to the surface of activated neutrophils. Using a fluorescent flow cytometry assay, we showed that an aptamer inhibitor of elastase also binds preferentially to activated neutrophils. We then tested the ability of the aptamer to image inflammation *in vivo* in a rat reverse passive Arthus reaction model. The aptamer achieved a peak target-to-background (T/B) ratio of 4.3 ± 0.6 in 2 hours. IgG, which is used clinically to image inflammation, took a longer time to achieve a lower T/B: 3.1 ± 0.1 at 3 hours. The difference in T/B values is due to the faster clearance of the aptamer signal from the blood pool.

Conclusions: It is feasible to apply aptamer ligands for use in diagnostic imaging, where they may offer significant advantages over monoclonal antibodies and other reagents.

Address: NeXstar Pharmaceuticals, Inc., 2860 Wilderness Place, Boulder, CO 80301, USA.

Correspondence: Drew Smith
E-mail: dsmith@nexstar.com

Key words: aptamer, diagnostic imaging, elastase, inflammation

Received: **4 August 1997**
Revisions requested: **27 August 1997**
Revisions received: **18 September 1997**
Accepted: **19 September 1997**

Chemistry & Biology November 1997, 4:809–816
http://biomednet.com/elecref/1074552100400809

Introduction

The development of SELEX technology has enabled the generation of nucleic acid ligands, known as aptamers, to a wide variety of target molecules [1,2]. These ligands are comparable to monoclonal antibodies in respect to their affinity and specificity, thus suggesting their possible use in therapeutic and diagnostic applications [3–5]. A particular application for which aptamers might be well suited is diagnostic imaging. Antibodies are large molecules (~180 kDa), and are cleared very slowly from circulation. As a result, they access some biological compartments and targets slowly, or not at all; when they do bind their targets, their slow clearance may necessitate waiting for days before a significant signal emerges from the background of excess unbound ligand. Not only is this long waiting period inconvenient, it limits the usefulness of imaging technology in diagnosing acute conditions, and precludes the use of short-lived radionuclides. In contrast, aptamers are much smaller (~10 kDa) and, in the absence of stabilizing formulations, are cleared quickly from the circulation. These properties led us to test the utility of an aptamer in inflammation imaging.

Infection and inflammation lead to the accumulation of neutrophils at the site of inflammation [6–8]. There, a variety of stimuli cause the release of neutrophil granules into the extracellular space [9]. Among the contents of these granules is neutrophil elastase, a serine protease that can degrade a variety of proteins, including those of host connective tissue. Because of its potency, elastase activity is highly localized to the neutrophil vicinity by high concentrations of α-1 proteinase inhibitor (α-1 PI) [10–13]. In addition, elastase activity has been reported to be stably bound to the neutrophil surface [14,15]. Thus, despite the fact that neutrophil elastase is a soluble protein, it appears to be sufficiently localized to be a plausible target in diagnostic imaging of inflammation.

We have described the isolation and characterization of aptamers that are highly potent and specific irreversible inhibitors of neutrophil elastase [16,17]. We used a method known as 'blended SELEX', in which a small, weakly reactive reversible inhibitor of elastase (a valyl diphenyl ester phosphonate) was incorporated into a randomized nucleic acid library. This method endows the library with a chemical function that forms a covalent bond with the active-site serine of elastase. By using the SELEX process of iterative selection and amplification, the nucleic acid sequences that best promote the covalent reaction of the valyl phosphonate moiety with elastase were identified. These inhibitors inactivate elastase with rate constants of $1\text{–}3 \times 10^8$ M^{-1} min^{-1}, nearly two orders of magnitude faster than peptide-based phosphonate inhibitors [16,18]. In addition to inhibiting elastase free in solution, we showed that these aptamers are highly effective at blocking degradation of elastin particles by activated neutrophils. Recently, we have also shown that our elastase aptamer reduces lung injury in a rat alveolitis model [19].

Here, we began our imaging studies by characterizing the interaction of the aptamers with neutrophils by fluorescence

Figure 1

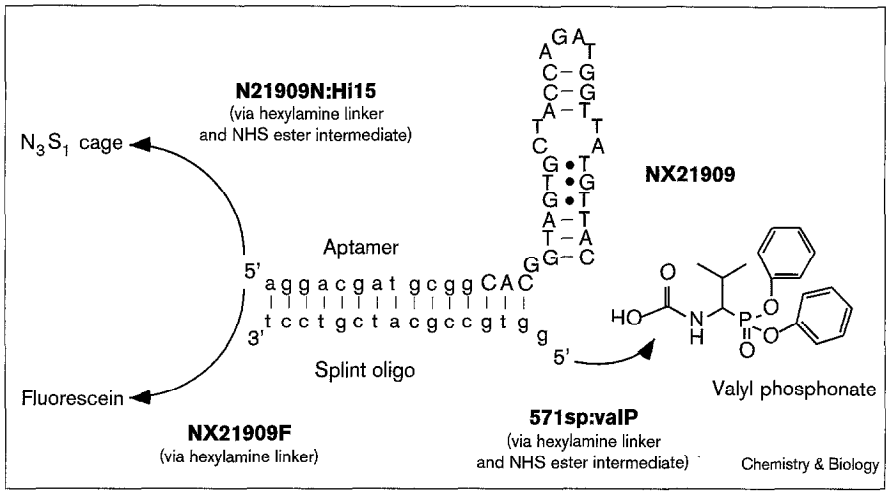

An aptamer inhibitor of elastase (NX21909). The inhibitor is composed of two annealed DNA oligonucleotides. The 'splint' oligonucleotide (splint oligo) is modified at the 5′ end with the valyl phosphonate inhibitor of elastase to form 571sp:valP. The active-site serine of elastase attacks the phosphorus atom, displacing a phenyl group to form a serine–phosphonate ester. The aptamer component of the inhibitor is a DNA sequence whose selection is described in [16]. This oligonucleotide was modified for imaging experiments by addition of fluorescein, to produce NX21909F, or a peptide 'cage', to produce N21909N:Hi15, at its 5′ end.

flow cytometry. We found that the elastase inhibitor binds to activated neutrophils from both humans and rats, and that there is a linear correlation between elastase activity and fluorescence intensity. We tested imaging *in vivo* in a rat model of the reverse passive Arthus reaction induced by immune complex deposition. Using region-of-interest (ROI) analysis, we found a target-to-background ratio of 4.3 ± 0.6 at 2 h after administration of the elastase aptamer, compared to a ratio of 3.1 ± 0.1 at 3 h for IgG, which is used clinically as an inflammation imaging agent [20–22]. These results indicate that aptamer ligands may be of value in diagnostic imaging.

Results and discussion

Flow cytometry analysis of neutrophil labeling

The potential utility of elastase inhibitors as imaging agents was suggested to us by reports that elastase is bound to the surface of activated neutrophils. We first asked whether our aptamer inhibitor (Figure 1, NX21909) could specifically label activated neutrophils *in vitro*. Flow cytometry (FACS) was used to detect binding of a fluorescently labeled aptamer (Figure 1, NX21909F) to human neutrophils. These experiments show that the elastase inhibitor aptamer does generate a strong fluorescence signal, relative to autofluorescence, on activated neutrophils. Furthermore, the fluorescence intensity is strongly correlated with the level of elastase activity induced (Figure 2), consistent with the hypothesis that elastase is a binding target of the aptamer on the neutrophil cell surface. Figure 2 also shows that there is a significant level of non-specific binding by a control DNA (30N7), and that immune complex activation induces somewhat higher cell binding relative to elastase activity than do other modes of activation.

Binding of elastase and control oligonucleotides to activated live neutrophils is linear with respect to DNA concentration, and is not saturable in the range of concentrations studied (Figure 3, circles). Some or all of this binding could be the result of endocytotic uptake of DNA [23]. We evaluated the possible contribution of such active mechanisms of DNA binding by determining binding to fixed cells (Figure 3, squares). Binding of both DNAs is

Figure 2

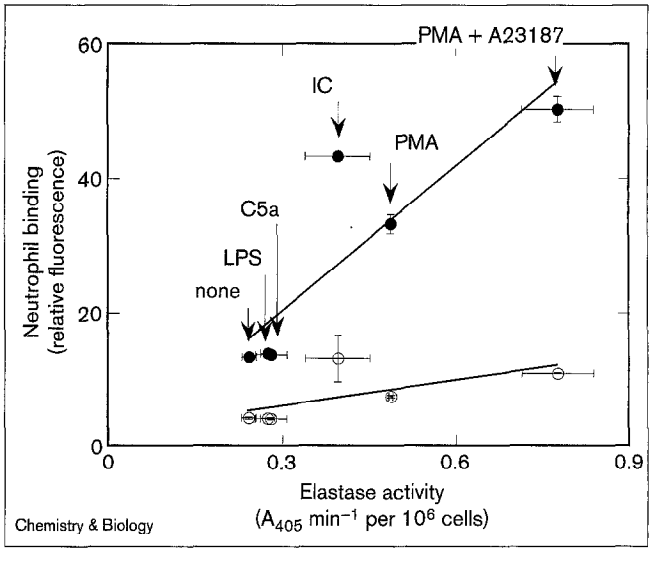

Correlation between elastase activity and neutrophil-labeling intensity. Human neutrophil preparations were activated by the indicated compounds, and assayed in parallel for elastase activity (x axis) and neutrophil binding (y axis). Closed circles, NX21909F; open circles, 30N7 (the control pool of oligonucleotides that has 30 randomized nucleotides between the same 5′ and 3′ PCR primer binding sites as the parent library from which NX21909 was selected). Bars indicate standard errors of the mean for three determinations, line is a linear regression by least-squares analysis. R^2 (NX21909F) = 0.76, $P < 0.05$; R^2 (30N7) = 0.44, $P > 0.1$. LPS, lipopolysaccharide; C5a, complement factor 5a; IC, immune complex; PMA, phorbol myristyl acetate; A23187, calcium ionophore A23187.

Figure 3

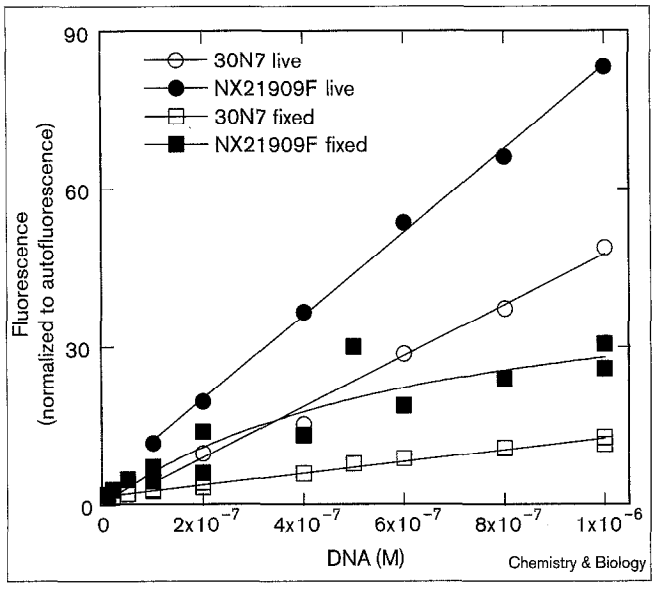

DNA binding to live and fixed activated neutrophils. Neutrophils were activated with phorbol myristyl acetate (PMA) for 30 min at 37°C. One portion was fixed in 3% formaldehyde/0.25% glutaraldehyde/phosphate-buffered saline (PBS), while the unfixed portion was processed in parallel. DNAs were added at the indicated concentration to 2×10^5 cells in 0.4 ml Hank's balanced saline solution (HBSS), and allowed to bind for 30 min at 37°C. Theoretical lines are linear regressions for all but 'NX21909F fixed', which was found to fit better to a hyperbolic curve (*r*-values 0.929 versus 0.909).

Figure 4

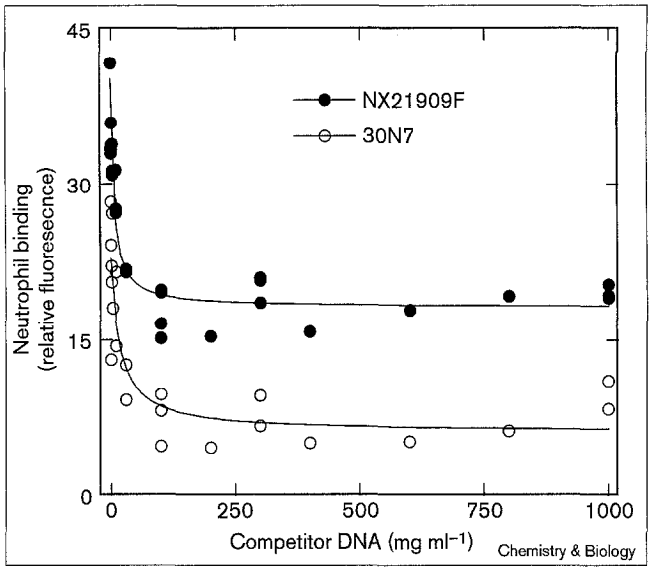

Competition for neutrophil labeling by non-specific DNA. Elastase aptamer (NX21909F) or randomized control (30N7) were at 30 nM, mixed with 10^5 human neutrophils and 0.1 μg ml^{-1} PMA in 0.4 ml total volume. Sheared denatured herring sperm DNA was included at the indicated concentrations. The data are fitted to a theoretical curve for partial competitive inhibition, $y = F_{max}(1 + (\beta[I]/K_i)/(1 + [I]/K_i))$, where F_{max} is fluorescence in the absence of inhibitor, β is the fraction of uninhibited fluorescence remaining at infinite inhibitor concentration, and K_i is the constant for half-maximal inhibition [36]. By this analysis, competitor DNA has a similar inhibition constant for both the elastase aptamer and the control (~10 μg ml^{-1}). However, whereas 0.73 (± 0.07) of the control DNA fluorescence can be competed away, only 0.55 (± 0.04) of the elastase aptamer fluorescence can be competed.

reduced for fixed cells, and binding by NX21909 appears to plateau at concentrations $> 5 \times 10^{-7}$ M, suggesting that binding to the neutrophil cell surface is being saturated. Fixation has different effects on binding by the DNAs, reducing binding by 4.4-fold for the control, against 1.9-fold (below 5×10^{-7} M) for the elastase aptamer. This result is consistent with the hypothesis that the elastase aptamer binds to activated neutrophils by specific, as well as non-specific, mechanisms.

We further characterized the nature of aptamer binding to neutrophils by adding denatured herring sperm DNA as a non-specific competitor (Figure 4). For both the elastase aptamer and the control oligonucleotide, binding to neutrophils shows partial competition. We interpret these data in terms of three modes of binding: (1) A non-specific, saturable component. This component is represented by the portion of the curves between 0–100 μg ml^{-1} herring sperm DNA where binding is competed away in a dose-dependent fashion; (2) A non-specific, non-saturable component. This component is represented by the plateau regions of the curves, above 100 μg ml^{-1} herring sperm DNA, and may result from active uptake of DNA into neutrophils [23]; (3) Specific binding to elastase. This is the binding by the elastase aptamer that cannot be competed by herring sperm DNA, and is represented by the differences in the plateau levels of binding by the control and elastase oligonucleotides. Although these data are open to other mechanistic interpretations, the results are compatible with the conclusion that the elastase aptamer binds activated neutrophils with a strong signal and some degree of specificity.

We determined cell-binding specificity of aptamer by measuring binding to the peripheral blood mononuclear cell (PBMC) fraction alone and in the presence of neutrophils. PBMCs activated by phorbol myristyl acetate (PMA) are labeled by the elastase aptamer with an intensity 0.15 ± 0.1 times that of neutrophils, while the 30N7 control oligonucleotide labels PBMCs at 0.23 ± 0.2 times the neutrophil intensity. This result is consistent with reports that PBMCs express low levels of elastase [24]. They do not significantly reduce the intensity of neutrophil labeling, however, when present at up to fivefold excess over neutrophils (data not shown). We also evaluated the effects of plasma on neutrophil labeling. Plasma contains high levels of α-1 PI, which can compete with the elastase aptamer for free elastase in solution (data not shown), and so could block binding to neutrophils. Addition of plasma at up to

10% of volume does reduce labeling to about 60% of the intensity in the absence of plasma (not shown). This effect, however, does not appear to be due to competition from α-1 PI, which can be added at 100-fold excess (1 μM concentration) over the elastase aptamer without reducing labeling intensity (data not shown). This result is consistent with that of Owen *et al.* [15], who found that α-1 PI was unable to inhibit surface-bound elastase. It is likely that the reduction of aptamer binding is due to degradation by plasma nucleases.

As we intended to use rat as a model system, we also examined binding to rat neutrophils. The elastase inhibitor used in these studies inactivates partially purified rat neutrophil elastase with a second-order rate constant of 1.1×10^7 M^{-1} min^{-1} [19]. This rate is about a third of that for the inactivation of human neutrophil elastase. As with human neutrophils, the elastase aptamer labels rat neutrophils in a dose- and activation-dependent fashion, but does so at an intensity only 0.2–0.5 that of human neutrophils. This lesser intensity is consistent with the relatively low levels of elastase found in rat neutrophils [25].

To summarize, these *in vitro* experiments show that the elastase aptamer binds to activated neutrophils from both rats and humans, and only weakly to quiescent neutrophils or to lymphocytes. The intensity of the binding signal correlates with elastase activity, although there is a significant non-specific, non-saturable binding component. Binding can take place in the presence of plasma, albeit with a significant reduction in signal. On the basis of these findings, we thought it plausible that an imaging signal could be generated at an inflammatory locus *in vivo*.

In vivo imaging

We induced a reverse passive Arthus (RPA) reaction in rats as our inflammation model [26]. Deposits of immune complexes were formed by intradermal injection of rabbit anti-bovine serum albumin (BSA) IgG in one forelimb, followed by intravenous tail vein injection of BSA. This model was preferred because our *in vitro* work showed that immune complexes stimulated elastase release and led to neutrophil labeling (Figure 2), whereas other inflammatory stimuli such as bacterial lipopolysaccharide (LPS) and complement fragment C5a did not. Visual inspection of the RPA reaction site showed marked swelling and reddening of the skin beginning 1–1.5 h post-injection, reaching a maximum at 3–3.5 h, which was sustained for ≥ 8 h. Histological analysis of skin sections at the site of the RPA reaction shows a large influx of neutrophils (Figure 5). Control injections of saline in the opposite forelimb caused no swelling, nor was there any accumulation of neutrophils.

^{99m}Tc is a gamma-emitting radionuclide that has a 6 h half-life and an energy emission spectrum which is ideal for imaging applications. Imaging agents were labeled with ^{99m}Tc and given by intravenous injection 3.5–4 h after induction of inflammation. The agents were the elastase aptamer (NX21909), a negative control aptamer (NX303), and rat IgG as a positive control. Rats were imaged in 10 min frames continuously for 40 min under anesthesia, then returned to their cages. Additional 10 min frames were taken every hour up to 4 h after administration of imaging agent.

A comparison of the elastase aptamer with the control aptamer and IgG at 10, 30, 60 and 120 min is shown in Figure 6. IgG, as expected, displays increased intensity in the RPA forelimb compared with the saline control. Clearance from circulation is slow, leading to high background intensity in the peripheral tissues. The non-specific control aptamer NX303 displays increased intensity in the RPA forelimb relative to the saline control. This apparent

Figure 5

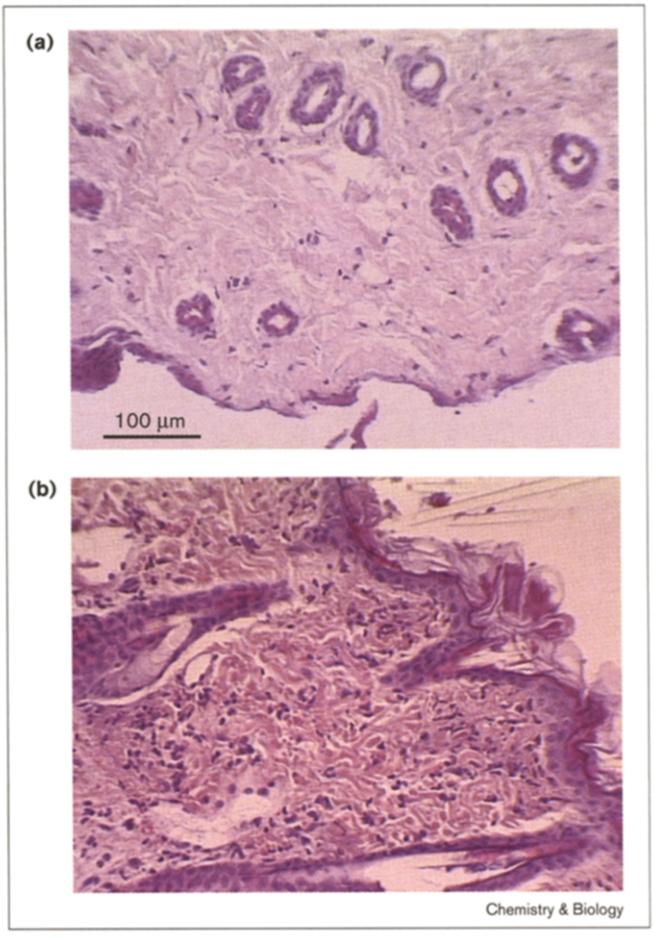

Histological analysis of the reverse passive Arthus reaction. Skin samples were excised from the sites of injection of saline **(a)**, or anti-BSA **(b)**, fixed in formalin, embedded in paraffin, sectioned and stained with hematoxylin and eosin. Neutrophils are the darkly stained cells that infiltrate the tissues. Magnification is × 20.

Figure 6

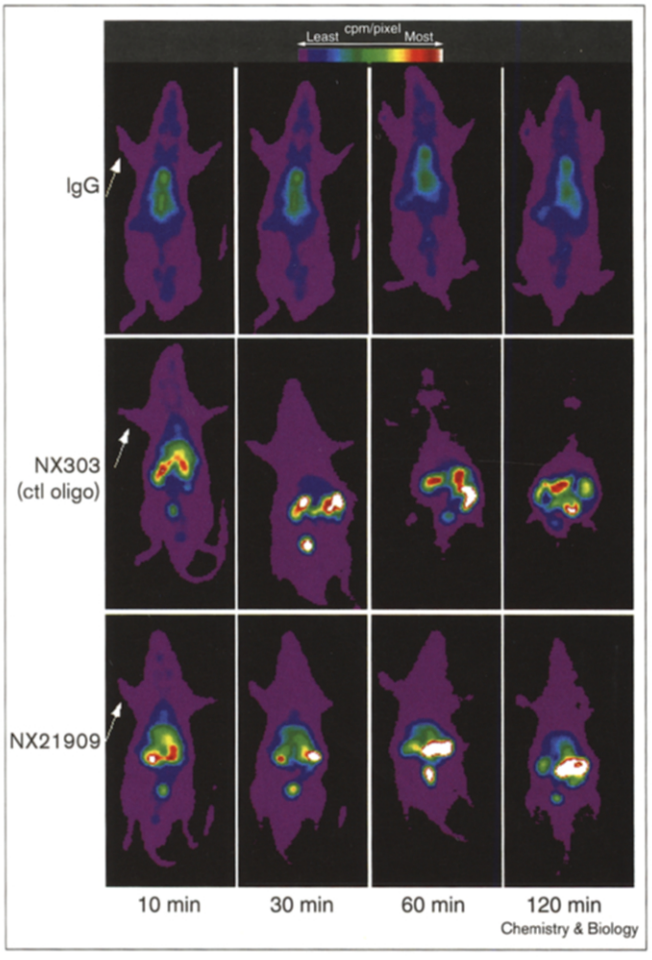

Inflammation imaging by NX21909 and IgG. A time series is shown in which the left forelimb of each rat is the site of the RPA reaction, indicated by the arrow, and the right forelimb is the background control (saline injection). Images were captured on a 256 × 256 pixel matrix. Images were smoothed, and color intensities normalized to total counts in the frame: purple, $> 3 \times 10^{-6}$ of the total counts per pixel; green, $> 3 \times 10^{-4}$ of the total counts per pixel; red, $> 3 \times 10^{-3}$ of the total counts per pixel; white, $> 10^{-2}$ of the total counts per pixel.

Figure 7

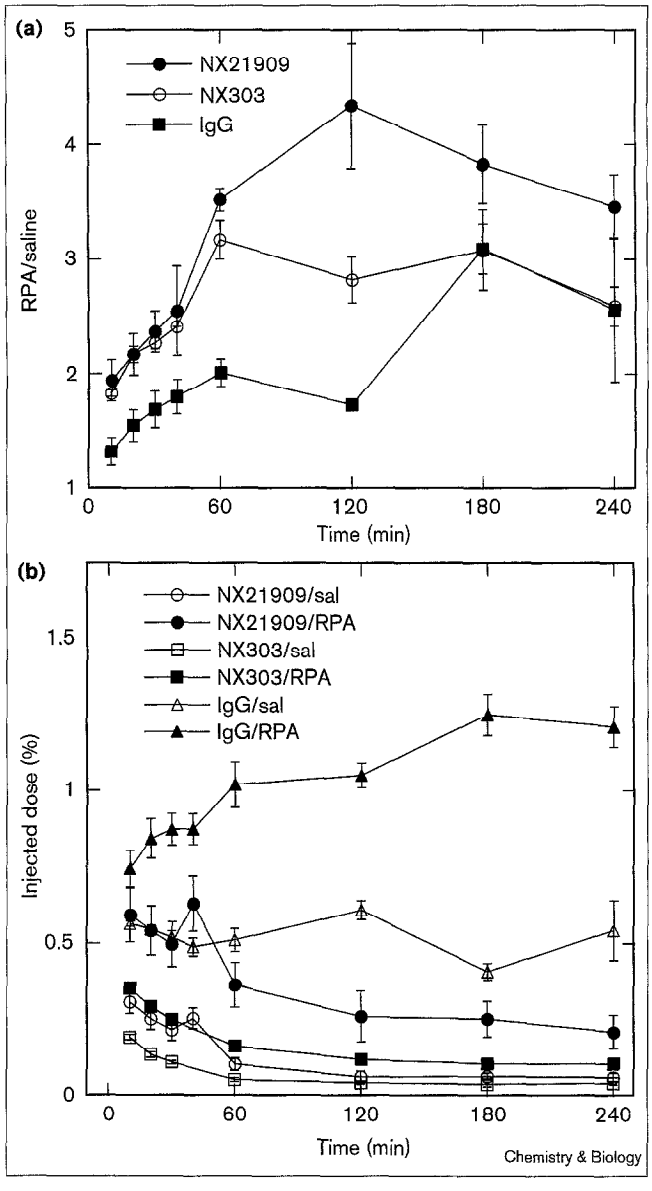

Quantification of imaging signal. **(a)** Target-to-background ratios were computed as the quotient of counts in the RPA forelimb to those in the saline forelimb. Bars indicate the s.e.m. For the elastase aptamer NX21909, $n = 7$; for the control oligo NX303, $n = 5$; for the positive control IgG, $n = 3$. For four rats each, NX21909 and NX303 were blinded and coded before injection, to eliminate bias from the ROI analysis. There was no significant difference in computed T/B between the four blind and three open experiments done with NX21909 ($P > 0.98$ by paired t-test analysis), so both data sets were combined. The overall level of significance for the difference between the NX21909 and NX303 data sets is $P = 0.023$. For the difference between NX21909 and IgG, $P < 0.01$. **(b)** The percent injected dose was calculated from the counts in the ROI as a percent of counts in the whole rat at the initial time of 10 min, corrected for decay.

binding may be due to increased blood flow, and to non-specific binding by neutrophils, as was shown *in vitro*. The elastase aptamer NX21909 shows greater intensity than the control oligonucleotide in the RPA forelimb, and persists in this forelimb longer than the control. In contrast to IgG, clearance from circulation is rapid, so that background intensity in peripheral tissues is low.

Target-to-background (T/B) ratios were determined by ROI analysis: the c.p.m. in the injection region (between the elbow and wrist) were quantified and expressed as the ratio of c.p.m. in the RPA site to those at the saline injection site (Figure 7a). The T/B ratio of the IgG-positive control rises slowly to a level of ~3 at 3–4 h. This result is quantitatively similar to results reported elsewhere [20,22].

The T/B ratio of the elastase aptamer (NX21909) rises much more quickly to a higher maximum of ~4 at 2 h, then begins to decline. A significant signal is also shown

by the negative control aptamer (NX303), and the two aptamers are difficult to distinguish by inspection, especially in the early portions of the time course. This result mirrors the non-specific binding to activated neutrophils *in vitro* (Figures 2,3,4). The T/B ratio of the elastase aptamer is significantly greater than in the negative control over the course of the experiment ($P = 0.023$ by paired *t*-test analysis). Although capillary leak or non-specific uptake of DNA probably contributes to the imaging signal, this difference indicates that elastase-binding activity makes a significant contribution as well.

Analysis of the total c.p.m. at the inflammation site shows fundamental differences in the behavior of the elastase aptamer and IgG (Figure 7b). The initial levels of IgG and elastase aptamer in the RPA forelimb are similar, but IgG accumulates slowly over time, whereas the elastase aptamer decreases. The superior T/B ratios achieved by the elastase aptamer are due to its very rapid clearance from the non-inflamed forelimb. By contrast, there is little or no clearance of IgG from the non-inflamed forelimb.

The results demonstrate the potential feasibility of using aptamers as reagents for diagnostic imaging. Like monoclonal antibodies, aptamers bind tightly and specifically to target molecules. Monoclonal antibodies are handicapped as imaging agents by their slow clearance rate: the time required to achieve a significant T/B ratio is often several days [27,28]. Aptamers, being nucleic acids, are cleared quickly from circulation, resulting in low background levels and high T/B ratios. The particular formulation used in this study, unmodified and unprotected DNA, is cleared rapidly, and is also highly susceptible to plasma nuclease degradation. Specific targeting of an inflammation site was still attained, despite minimal opportunities for the aptamer to interact with its target. It is likely that the use of more stable chemistries and formulations [29,30] will further optimize the imaging signal.

Two critical issues involved in evaluating aptamers as imaging agents are the specificity of the signal and its intensity. Aptamer ligands generally display high specificity [30–32], and the elastase aptamer has also shown high specificity *in vitro* [16]. We found a significant non-specific binding component in the cell-binding assay (Figures 3,4) and in RPA imaging (Figure 7). There have been several reports of DNA-binding activity by neutrophils [23,33,34], which may account for the non-specific binding. Binding of DNA by the Mac-1 protein, which is upregulated upon neutrophil activation, results in the internalization of DNA [23]. This type of binding may account for our observations that binding of NX21909 is only partly competed by herring sperm DNA.

These non-specific mechanisms cannot account for all of the binding by the elastase inhibitor NX21909. Both *in vitro* and *in vivo*, binding by NX21909 to the targeted cells or tissues is significantly greater than that to non-specific controls. The *in vitro* data (Figures 3,4) show that non-specific binding by neutrophils cannot account for all of the binding by NX21909; the *in vivo* data (Figure 7) show that neither this mechanism nor vascular leak can account for all of the imaging signal generated by NX21909.

Although imaging, as measured by T/B ratio is twofold to threefold higher for NX21909 than for IgG at 120 min (Figure 7a), the absolute intensity of the signal is twofold to threefold lower (Figure 7b). One probable reason for the low signal intensity is the relatively low levels of elastase expressed by rat neutrophils relative to human neutrophils [35]. Rat neutrophils instead express high levels of cathepsin G, which does not bind the elastase aptamer [19]. These low levels of elastase expression may not limit signal intensity in other animal models or in humans.

Other factors that may limit signal intensity are the pharmacokinetic and biodistribution properties of the aptamer, which prevent it from accumulating in the target tissue. Inspection of imaging experiments indicates that much of the radioactivity is initially taken up by the liver, then excreted into the gut. Significant accumulation in the kidneys and bladder is also evident. This pattern of biodistribution could interfere with some inflammatory imaging applications, such as diagnosis and localization of inflammatory bowel disease. Further progress in the development of aptamer imaging technology will focus on finding more stable formulations.

Significance

An aptamer irreversible inhibitor of neutrophil elastase was successfully used for diagnostic imaging of inflammation in rats. The aptamer was compared with IgG, which is used clinically in diagnostic imaging of inflammatory diseases. The aptamer achieved a significantly higher target-to-background ratio in less time than IgG. This ratio was achieved primarily by the rapid clearance of the aptamer from the peripheral circulation. Although preliminary, these results indicate that aptamer technology may be successfully applied to diagnostic imaging.

Materials and methods

Oligonucleotides

The core elastase inhibitor NX21909 is diagrammed in Figure 1. The fluorescently labeled derivative of the inhibitor, NX21909F, has fluorescein at the 5′ end of the aptamer moiety, and was synthesized and HPLC-purified by Operon. This derivative inactivates human neutrophil elastase (hNE) at the same rate as its parent ($3 \times 10^7\ M^{-1}\ min^{-1}$), as determined by the progress curve method. The ligand for *in vivo* imaging, designated NX21909N, was first synthesized as the 5′hexylamine derivative of NX21909 (Macromolecular Resources), and purified by reverse-phase HPLC. A peptide N_3S_1-type Tc-binding cage was attached via the amine linker of NX21909N via an NHS-ester reaction in dry DMSO/5% triethyl amine (TEA). The product of this reaction, NX21909N:Hi15, was purified by reverse-phase HPLC. This derivative

is significantly less active than its parent, with an inactivation rate constant of 6×10^6 M^{-1} min^{-1} against hNE. The negative controls in all *in vitro* experiments were 30N7 (a pool of oligonucleotides that has 30 randomized nucleotides between the same 5′ and 3′ PCR primer binding sites as the parent library from which NX21909 was selected) as the aptamer strand, annealed to a splint oligonucleotide strand having a fluorescein attached via a 5′ hexylamine linker, in place of the valyl phosphonate moiety of the inhibitor molecules. For *in vivo* experiments, the DNA oligonucleotide NX303 [30] with a Hi15 cage attached at the 5′ end was used as a negative control. This oligonucleotide binds human, but not rat, L-selectin [30]. Inhibitors and controls were prepared by mixing equimolar amounts of aptamer and splint oligonucleotides in Hank's balanced saline solution (HBSS) heating to 65°C and slowly cooling to 37°C.

Technetium labeling

For oligonucleotides, 100 μl (10 mCi) of [^{99m}Tc]sodium pertechnetate (Syncor) was added to 100 μl 2 M sodium tartrate/0.3 M Tricine pH 7.4 with 3 μl 0.5 M tricarboxyethyl phosphine (TCEP, Pierce) as a reducing agent, and incubated at 60°C for 10 min. Oligonucleotide (0.5–1 nmol) was added, along with an additional 1 μl 0.5 M TCEP, and incubation at 60°C was continued for 10 min. HBSS/0.01% BSA (100 μl) was added, the reaction was transferred to a Microcon 30 kDa MWCO ultrafiltration cartridge and centrifuged to near-dryness. The sample was resuspended and recentrifuged three times in 300 μl HBSS, then resuspended in 200 μl HBSS. HPLC analysis showed that > 95% of the radioactivity is associated with the oligonucleotide (not shown). Specific activities were typically 0.7–1.5 mCi $nmol^{-1}$ oligonucleotide.

IgG (rat, Sigma) was labeled by mixing 100 μl of 10 mg ml^{-1} IgG with 900 μl HBSS and 150 mg dithiothreitol (DDT), and incubating at room temperature for 30 min. Any precipitates were removed by centrifugation through a Spin-X 0.45 μm cellulose acetate filter cartridge. DTT was removed by centrifugation through Microcon 30 kDa MWCO ultrafiltration cartridges, washing with 3×400 μl HBSS, and recovering in 100 μl volume. [^{99m}Tc]sodium pertechnetate was activated as described above, then added to the IgG and incubated for 15 min at room temperature. Free radiolabel was removed by ultrafiltration as described above. Specific activities were 3–4 mCi mg^{-1} protein.

Neutrophil preparation

Blood samples (20 ml) drawn from human volunteers were layered on a discontinuous gradient of 12.5 ml each Histopaque 1077 and Histopaque 1119 (Sigma) in a 50 ml conical Falcon tube, and centrifuged in a swinging bucket rotor at 400 g for 30 min at room temperature. Neutrophils were drawn from the Histopaque 1077-1119 interface, and any contaminating red blood cells were hypotonically lysed by 30 s of vortexing in 3 ml ice-cold water. Lysed cells and Histopaque were removed by washing cells three times in 20 ml HBSS containing no Ca^{2+} or Mg^{2+}. Neutrophils were resuspended in the same buffer, and their number and viability were determined by counting in 0.2% Trypan Blue. Neutrophils were fixed for binding experiments in 3% paraformaldehyde/0.25% glutaraldehyde, following the procedure of [15].

Femurs were harvested from 3–5-month-old male Harlan Sprague-Dawley rats and placed in Ca/Mg-free HBSS. Within 10 min of harvesting, the ends of the femur were broken off and Ca/Mg-free HBSS was squirted through the bone with an 18-gauge needle until all stringy red bone marrow was collected into a 50 ml Falcon tube (45 ml). A 10 ml syringe (no needle) was used to break up the bone marrow by aspiration. The mixture was then strained through a 2360 Falcon cell strainer, and cells were pelleted by centrifugation at 700 g for 10 min. The pellets were resuspended in 2 ml of E-Lyse (Cardinal Associates), vortexed for 1 min and re-pelleted, then resuspended in Ca/Mg-free HBSS. The resuspended cells were passed through another 2360 Falcon cell strainer to remove fat precipitates and then counted via Trypan Blue viable staining. The fraction of mature neutrophils in the preparation was 30–40%.

Inhibition assays

Elastase activity of 10^5 neutrophils was determined by the progress curve method in a colorimetric assay, using *N*-methoxysuccinyl-Ala-Ala-Pro-Val-*para*-nitroanilide as a substrate [17]. LPS (lipopolysaccharide from *E. coli*) was at 0.1 μg ml^{-1}; C5a was at 0.1 μg ml^{-1}; PMA was at 0.1 μg ml^{-1}; calcium ionophore A23187 was at 0.5 μg ml^{-1}; IC (immune complex) was formed by mixing BSA at 80 μg ml^{-1} and anti-BSA IgG at 800 μg ml^{-1}.

Cytometry

Fluorescein-labeled nucleic acids (usually at 30 nM), activator (usually PMA at 10 ng ml^{-1}) and 10^5 neutrophils were mixed in 0.4 ml HBSS at 37°C, and allowed to equilibrate for 10 min. Cells were gated and fluorescence was quantified using a FACScalibur (Becton-Dickinson) fluorescence-activated cell sorter. 10^4 events in the neutrophil gate were collected for each sample, and fluorescence intensity was calculated as the geometric mean of all events within the gate. Data are reported as the quotient of intensities in the presence and absence of the fluorescein-tagged ligands.

Inflammation imaging

Male Harlan Sprague-Dawley rats, 250–300 g were anesthetized and given intradermal injections of 33 μl anti-BSA (rabbit IgG fraction, Cappel) (6 mg ml^{-1}) or HBSS on the right and left forelimbs, respectively. BSA (200 μl of 50 mg ml^{-1}) was given by tail vein intravenous injection at the same time. Radiolabeled imaging compounds at approximately 0.5 mCi, were administered by tail vein intravenous injection 3.5 h after anti-BSA administration.

Animals were imaged on a Siemens LEM+ gamma camera under continuous anesthesia for 40 min, then returned to their cages to recover. Additional images were taken at 1, 2, 3 and 4 h after administration of the imaging agent. After 4 h, the rats were killed by asphyxiation under CO_2, and skin samples of approximately 1 cm^2 were taken from the forelimb injection sites for histochemical analysis. Image presentation and analysis were performed using NucLear MAC v2.9 software (Scientific Imaging, Inc.). An ROI of approximately 1 cm diameter was drawn around the injection sites on the forelimb. For the time periods in which the rats were under continuous anesthesia, and thus immobilized, this ROI was copied to all frames in the image file, providing a consistent size and shape for each measurement. The total number of counts in each ROI was evaluated, corrected for decay, and normalized to the nominal injected dose.

In blind experiments, two aliquots each of radiolabeled NX303 and NX21909, containing identical amounts of radioactivity, were distributed to numbered tubes by Daniel Schneider. The matching of the tube numbers with the oligonucleotide identity was not made until the ROI analysis was completed.

Acknowledgements

We thank Kristi Vrkljan for HPLC purification, Jim Heil and Stefan Hilger for synthesis of the cage NHS-ester, Anna Magallanez for histology, and Dwight Henninger and Paul Schmidt for critical reading of the manuscript.

References

1. Ellington, A. & Szostak, J. (1990). In vitro selection of RNA molecules that bind specific ligands. *Nature* **346**, 818-822.
2. Tuerk, C. & Gold, L. (1990). Systematic evolution of ligands by exponential enrichment: RNA ligands to bacteriophage T4 DNA polymerase. *Science* **249**, 505-510.
3. Gold, L. (1995). Oligonucleotides as research, diagnostic, and therapeutic agents. *J. Biol. Chem.* **270**, 13581-13584.
4. Gold, L., Polisky, B., Uhlenbeck, O. & Yarus, M. (1995). Diversity of oligonucleotide functions. *Annu. Rev. Biochem.* **64**, 763-797.
5. Ellington, A.D. (1994). RNA selection. Aptamers achieve the desired recognition. *Curr. Biol.* **4**, 427-429.
6. Varani, J. & Ward, P.A. (1989). Mechanisms of neutrophil-dependent and neutrophil-independent endothelial cell injury. *Biol. Signals* **3**, 1-14.

7. Weiss, S.J. (1989). Tissue destruction by neutrophils. *N. Engl. J. Med.* **320**, 365-376.
8. Repine, J. (1992). Scientific perspectives on adult respiratory distress syndrome. *Lancet* **339**, 466-469.
9. Wright, D. (1988). Human neutrophil degranulation. *Methods Enzymol.* **162**, 538-551.
10. Weiss, S.J. & Regiani, S. (1984). Neutrophils degrade subendothelial matrices in the presence of alpha-1-proteinase inhibitor. Cooperative use of lysosomal proteinases and oxygen metabolites. *J. Clin. Invest.* **73**, 1297-1303.
11. Liou, T. & Campbell, E. (1995). Nonisotropic enzyme-inhibitor interactions: a novel nonoxidative mechanism for quantum proteolysis by human neutrophils. *Biochemistry* **34**, 16171-16177.
12. Rice, W.G. & Weiss, S.J. (1990). Regulation of proteolysis at the neutrophil–substrate interface by secretory leukoprotease inhibitor. *Science* **249**, 178-181.
13. Travis, J. & Salvesen, G. (1983). Human plasma proteinase inhibitors. *Annu. Rev. Biochem.* **52**, 655-709.
14. Allen, D.H. & Tracy, P.B. (1995). Human coagulation factor V is activated to the functional cofactor by elastase and cathepsin G expressed at the monocyte surface. *J. Biol. Chem.* **270**, 1408-1415.
15. Owen, C.A., Campbell, M.A., Sannes, P.L., Boukedes, S.S. & Campbell, E.J. (1995). Cell surface-bound elastase and cathepsin G on human neutrophils: a novel, non-oxidative mechanism by which neutrophils focus and preserve catalytic activity of serine proteinases. *J. Cell. Biol.* **131**, 775-789.
16. Charlton, J., Kirschenheuter, G.P. & Smith, D. (1997). Highly potent irreversible inhibitors of neutrophil elastase generated by selection from a randomized DNA-valine phosphonate library. *Biochemistry* **36**, 3018-3026.
17. Smith, D., Kirschenheuter, G., Charlton, J., Guidot, D. & Repine, J. (1995). *In vitro* selection of RNA-based irreversible inhibitors of human neutrophil elastase. *Chem. Biol.* **2**, 741-750.
18. Oleksyszyn, J. & Powers, J. (1991). Irreversible inhibition of serine proteases by peptide derivatives of (alpha-aminoalkyl)phosphonate diphenyl esters., *Biochemistry* **30**, 485-493.
19. Bless, N.M., *et al.*, & Ward, P.A. (1997). Protective effects of an aptamer inhibitor of neutrophil elastase in lung inflammatory injury. *Curr. Biol.* **7**, 877-880.
20. Babich, J.W., Graham, W., Barrow, S.A. & Fischman, A.J. (1995). Comparison of the infection imaging properties of a ^{99m}Tc labeled chemotactic peptide with ^{111}In IgG. *Nucl. Med. Biol.* **22**, 643-648.
21. Morrel, E.M., *et al.*, & Yarmush, M.L. (1990). Imaging infections with antibodies. A quantitative autoradiographic analysis. *J. Immunol. Methods* **130**, 39-48.
22. Barrow, S.A., Graham, W., Jyawook, S., Dragotakes, S.C., Solomon, H.F., Babich, J.W., Rubin, R.H. & Fischman, A.J. (1993). Localization of indium-111-immunoglobulin G, technetium-99m- immunoglobulin G and indium-111-labeled white blood cells at sites of acute bacterial infection in rabbits. *J. Nucl. Med.* **34**, 1975-1979.
23. Benimetskaya, L., *et al.*, & Stein, C.A. (1997). Mac-1 (CD11b/CD18) is an oligodeoxynucleotide-binding protein. *Nat. Med.* **3**, 414-420.
24. Campbell, E., Silverman, E. & Campbell, M. (1989). Elastase and cathepsin G of human monocytes. Quantification of cellular content, release in response to stimuli, and heterogeneity in elastase-mediated proteolytic activity. *J. Immunol.* **143**, 2961-2968.
25. Bray, M., McKearn-Smith, C., Metz-Virca, G., Bodmer, J. & Virca, G. (1989). Stimulated release of neutral proteinases elastase and cathepsin G from inflammatory rat polymorphonuclear leukocytes. *Inflammation* **11**, 23-37.
26. Warren, J.S., Johnson, K.J. & Ward, P.A. (1990). PAF and immune complex-induced injury. *J. Lipid Mediat.* **2** (suppl), S229-S237.
27. Pike, M.C. (1991). Imaging of inflammatory sites in the 1990s: new horizons, *J. Nucl. Med.* **32**, 2034-2036.
28. Oyen, W.J. & Corstens, F.H. (1995). Scintigraphic techniques for delineation of infection and inflammation. *Br. J. Hosp. Med.* **54**, 75-80.
29. Lin, Y., Qiu, Q., Gill, S. & Jayasena, S. (1994). Modified RNA sequence pools for in vitro selection. *Nucleic Acids Res.* **22**, 5229-5234.
30. O'Connell, D., *et al.*, & Varki, A. (1996). Calcium-dependent oligonucleotide antagonists specific for L- selectin. *Proc. Natl Acad. Sci. USA* **93**, 5883-5887.
31. Jellinek, D., *et al.*, & Janjic, N. (1995). Potent 2′-amino-2′-deoxypyrimidine RNA inhibitors of basic fibroblast growth factor. *Biochemistry* **34**, 11363-11372.
32. Jenison, R.D., Gill, S.C., Pardi, A. & Polisky, B. (1994). High-resolution molecular discrimination by RNA. *Science* **263**, 1425-1429.
33. McAfee, J.G. & Thakur, M.L. (1976). Survey of radioactive agents for in vitro labeling of phagocytic leukocytes. I. Soluble agents. *J. Nucl. Med.* **17**, 480-487.
34. Gabor, G. & Bennett, R.M. (1984). Biotin-labelled DNA: a novel approach for the recognition of a DNA binding site on cell membranes, *Biochem. Biophys. Res. Commun.* **122**, 1034-1039.
35. Mulligan, M.S., Desrochers, P.E., Chinnaiyan, A.M., Gibbs, D.F., Varani, J., Johnson, K.J. & Weiss, S. (1993). *In vivo* suppression of immune complex-induced alveolitis by secretory leukoproteinase inhibitor and tissue inhibitor of metalloproteinases 2. *Proc. Natl Acad. Sci. USA* **90**, 11523-11527.
36. Segel, I.H. (1975). *Enzyme Kinetics*. John Wiley & Sons, New York.